THE ASTROPHYSICAL JOURNAL, 424:L95–L98, 1994 April 1

THE DISTRIBUTION AND KINEMATICS OF ATOMIC CARBON NEAR THE GALACTIC CENTER

E. SERABYN, JOCELYN KEENE, D. C. LIS, AND T. G. PHILLIPS
California Institute of Technology, 320-47, Pasadena, CA 91125
Received 1993 August 30; accepted 1993 December 28

ABSTRACT

The central several parsecs of our Galaxy have been mapped in the 492 GHz $^3P_1 \rightarrow {}^3P_0$ fine-structure transition of C I with the Caltech Submillimeter Observatory. The observed region includes the entire southern half of the circumnuclear disk (CND) and part of its northern half. C I is found to be a good tracer of the outer parts of the CND, with an abundance close to that of CO. The high angular resolution (15″) of these observations, coupled with the low opacity of the C I line, provide a clear view of the disk's outer regions. The CND kinematics between radii of ~2.3 and 7 pc are found to be dominated by rotation, with a rotational velocity, 120 km s^{-1}, which is independent of radius. The implied central mass increases roughly linearly with radius, with, in the spherically symmetric case, a slope of $3.3 \times 10^6\ M_\odot$ pc^{-1}, reaching a total of $23 \times 10^6\ M_\odot$ at the CND's periphery.

Subject headings: galaxies: nuclei — Galaxy: center — ISM: atoms

1. INTRODUCTION

Circulating about the Galactic center at radii of ~1.4–7 pc (1 pc = 24″ for an 8.5 kpc distance to the Galactic center) is a torus of molecular and atomic gas, commonly referred to as the circumnuclear disk (CND; Genzel & Townes 1987), thought to be the source of material accreting toward our Galaxy's core. By means of its kinematics and excitation state, the CND has been used to probe the central gravitational and radiation fields. Results regarding the CND's excitation state (T_{ex} ranges from ~300 K near the CND's inner edge to ~100 K near its periphery; Genzel et al. 1985; Harris et al. 1985; Serabyn & Güsten 1986; Sutton et al. 1990) have been quite consistent, as have most observations of the disk kinematics, which show gas motions dominated by circumnuclear rotation (see, however, Gatley et al. 1986), with a rotational velocity approximately independent of radius (Serabyn et al. 1986; Güsten et al. 1987; Sutton et al. 1990). However, as some early observations of the CND (Harris et al. 1985; Lugten et al. 1986) showed lower velocities at large radii, some doubt as to the form of the rotation curve at Galactocentric radii $\gtrsim$3.5 pc persists (Güsten et al. 1987; Genzel 1989).

With the advent of high-frequency receivers at the Caltech Submillimeter Observatory (CSO), a new high spatial resolution probe of molecular clouds has become available, namely, the $^3P_1 \rightarrow {}^3P_0$ fine-structure transition of C I at 492 GHz. Earlier expected only at the photodissociated surfaces of molecular clouds, C I emission has in fact been found to arise throughout the bulk of most molecular clouds, being usually comparable in distribution to ^{13}CO (Phillips & Huggins 1981; Keene 1990). Thus, with the 15″ beam available at 492 GHz at the CSO, the C I line has the potential of being a probe not merely of the inner strongly photoilluminated portions of the CND, on which most studies of the CND have tended to concentrate, but also of its entire radial extent. In the following, we present C I observations which show that this is indeed the case, and use these data to examine the CND kinematics out to it periphery. Finally, we relate these kinematics to our Galaxy's central gravitational potential, which at these radii should be dominated by the distributed stellar component (Rieke & Rieke 1988; McGinn et al. 1989).

2. OBSERVATIONS AND RESULTS

The C I 1–0 line was observed on 1993 May 31 and June 1 and 4, with the SIS receiver described by Walker et al. (1992). T_{rx}(DSB) was 200 K, and T_{sys}(SSB) was, for a typical elevation angle of 40°, ~4000 K on the first two nights, during which we mapped most of the CND's southern half (south of Sgr A*, our Galaxy's central radio point source; Lo 1989), and ~8000 K on the third night, during which the map was extended slightly eastward and westward, and all of the spectra north of Sgr A* were measured. In total, 155 spectra were acquired on an (α, δ) grid with 15″ spacing and zero position coincident with Sgr A*. The pointing was checked on Jupiter. The back end was a 1024 channel acousto-optical spectrometer of bandwidth 560 MHz (340 km s^{-1}) centered at 0 km s^{-1} LSR.

Figure 1 shows a few representative C I spectra on the T_A^* scale. Conversion to T_{MB} requires division by the main-beam efficiency, 0.46 during our observations. The left-hand panel shows four "southern" spectra, while the right shows two "northern" spectra, as well as two spectra close to Sgr A*. All of these spectra show strong emission in the velocity range 0–80 km s^{-1} from the more extended "20 km s^{-1}" and "50 km s^{-1}" molecular clouds located along the same lines of sight (Brown & Liszt 1984). Although this velocity range consequently provides little useful information on the CND, outside this range the CND emission is easily discerned. The spectra south of Sgr A* all show the highly blueshifted emission which arises in the CND's southern half. At offset (−15, −150), near the CND's southern periphery, the CND component shows a line-of-sight velocity centroid of −114 km s^{-1}. The line-of-sight velocity decreases systematically in magnitude toward the center, until at (0, 0) the line appears only as a weak blue wing on the 50 km s^{-1} cloud emission. The C I line widths near the CND's southern periphery are only ~14–17 km s^{-1} FWHM, by far the narrowest seen in the CND. Closer to the center, the C I lines are broader, but in at least one location, (0, −90) the CND emission is seen to break up into narrower velocity components, indicating that the broad lines are due to overlapping clumps or filaments in the beam.

North of Sgr A*, CND emission is seen on the opposite side of the 20 and 50 km s^{-1} emission bands, at high positive

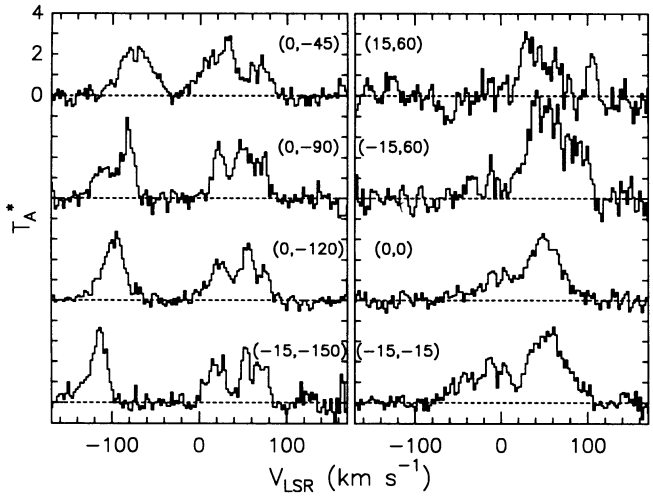

FIG. 1.—Selected spectra of C I in the CND. The channel width is 2.4 km s^{-1}. Offsets in (α, δ), in seconds of arc, are given in the panels.

velocities (Fig. 1). At offset (−15, 60) CND emission is seen in the range 80–100 km s^{-1}, still blended with the 50 km s^{-1} emission component, while at (15, 60) CND emission shows up as a resolved velocity component at +105 km s^{-1}. However, because of the limited extent of the region mapped north of Sgr A* and the lower signal-to-noise ratio of these spectra, it is not yet possible to estimate the full extent or maximum velocity of the CND's northern lobe. Therefore, this side of the CND will not be discussed further here, except to note that the C I distribution redward of 80 km s^{-1} generally corresponds well with that of CO.

Figure 2 (Plate L7) shows the full negative velocity data set, in the form of 20 km s^{-1} wide channel maps. Two separate kinematic features immediately stand out. The first is the circumnuclear disk, which at velocities near −100 km s^{-1} extends nearly 3′ southward from the center, an extent similar to that of CO and CS (Serabyn et al. 1986; Sutton et al. 1990). The highest negative velocities arises farthest from the center, and, as the velocity decreases, the emission perambulates toward the center, until at velocities near −50 km s^{-1} the emission begins to split, swinging around the center both to the east and to the west. Finally, in the −30 and −10 km s^{-1} channels, a reasonably well-defined ring of emission around, but centered slightly north of, Sgr A* is revealed, similar to the interferometric HCN map of Güsten et al. (1987). (The −10 km s^{-1} channel is slightly contaminated by a small region of unrelated emission due north of Sgr A* [Serabyn et al. 1986], as well as a possible ridge of C I emission extending to the southeast.)

These data have several implications. First, since the C I emission extends to radii of ∼170″, and shows no obvious enhancement near the CND's inner edge (∼35″ south of Sgr A*), the C I line must evidently arise throughout much of the bulk of the CND, and not merely within its inner photodissociation region. Second, the CND's lumpy appearance in both the spectra and the channel maps provides direct evidence for marked clumpiness or filamentation in the CND. Third, the comparatively narrow observed C I line widths imply that the large "turbulent" motions seen near the CND's inner edge (50–70 km s^{-1}; Güsten et al. 1987; Jackson et al. 1993) do not extend to larger radii.

The C I observations have also successfully resolved a second negative velocity feature, with different kinematics, from the bulk of the disk. This compact feature, located near offset (−60, −75) in the −70 to −10 km s^{-1} channel maps, will be referred to as the "negative longitude," or "$-l$," cloud because of its location close to the Galactic plane (at $\Delta l \approx -95''$ from Sgr A*). In Figure 2 this cloud is relatively stationary from channel to channel, advancing only slightly toward $-\alpha$ and $+\delta$ as its velocity increases from −70 km s^{-1} to −10 km s^{-1}. The $-l$ cloud thus does not share in the CND's obvious kinematic trend of shifting rapidly to higher δ with decreasing velocity, and so it is evidently not part of the CND. However, since the spectra near this cloud show more than one broad negative velocity component, its intrinsic structure and kinematics remain unclear.

Other than the CND and this $-l$ cloud, no other features at velocities more negative than −20 km s^{-1} are present in the entire area mapped in C I, in marked contrast to CO (Serabyn et al. 1986; Sutton et al. 1990). Because of its lower opacity, the C I line evidently discriminates very well in favor of the CND emission (and the two positive-velocity clouds). Indeed, a position-velocity plot (Fig. 3) along the CND major axis (at P.A. 6°), shows that the *only* feature present south of the center at negative velocities is the CND. This plot thus provides the clearest exposition of the kinematics of the outer parts of the CND acquired to date, for the dual reasons of low opacity in the C I line, and high angular resolution. Both of these factors also contribute to the extremely narrow C I line widths in the outer parts of the CND.

3. DISCUSSION

The column density of C I in the CND can be derived if the emission is optically thin (Keene 1990). Since the peak T_{MB} of the C I emission is only ∼8 K, while the excitation tem-

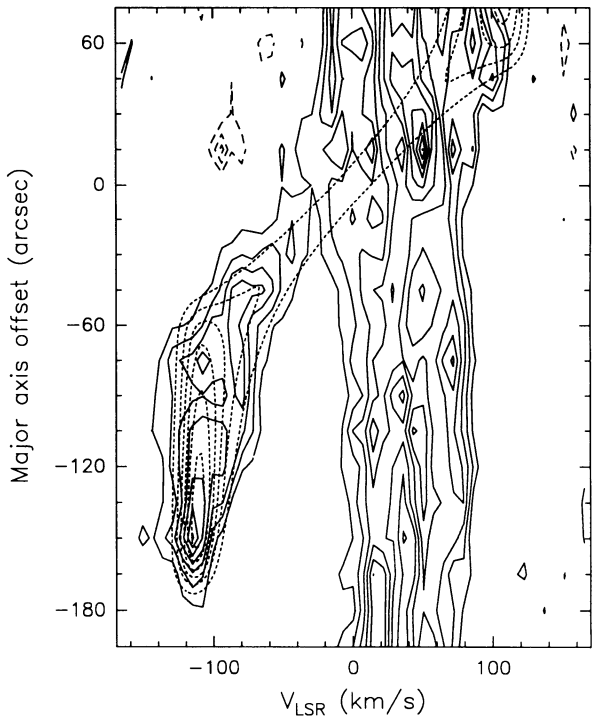

FIG. 3.—Position-velocity diagram along the disk major axis at P.A. = 6° (east of north). *Solid contours*: C I data, with contour levels of 0.5, 1.0, 1.5, ... K, in units of T_A^*. *Dashed contours*: disk model, with parameters as given in text.

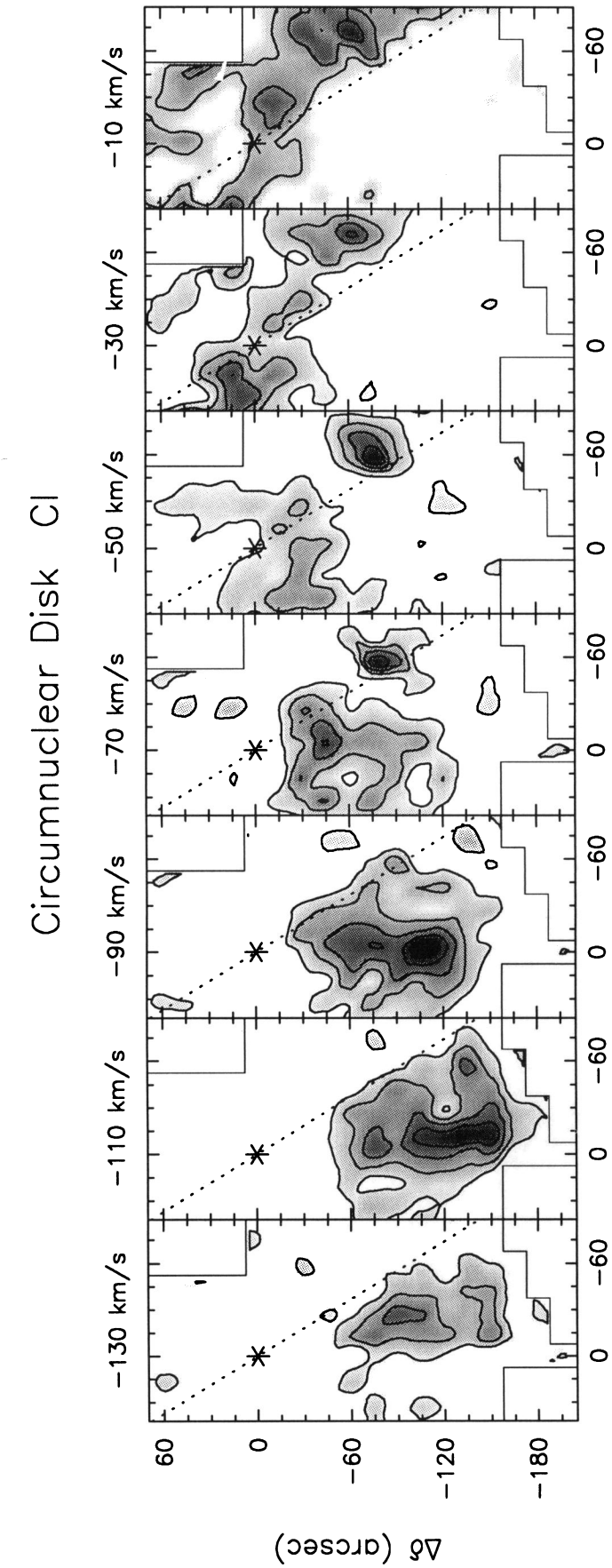

FIG. 2.—C I in the circumnuclear disk. Negative-velocity channel maps of the C I 492 GHz emission from the Galactic center. The channels are 20 km s^{-1} wide, and centered on the velocities given above the panels. The asterisk gives the location of Sgr A*, and the dashed line the true Galactic plane. The observed region is outlined in each panel by the boundary polygon. The contour levels are uniformly 8, 20, 32, 44, and 56 K km s^{-1}, except for the −10 km s^{-1} panel, for which the lowest contour has been omitted. The gray-scale range is 5–62 K km s^{-1}, except for the last map, where it is 10–62 K km s^{-1}. The rms noise is about 1 K km s^{-1} south of Sgr A*, and twice that to the north of Sgr A*.

perature is likely of order 100 K in the middle and outer parts of the CND (Sutton et al. 1990), where the C I emission originates, the emission is evidently either optically thin or highly clumped. Sutton et al. (1990) estimate the CO beam filling factor to be $\sim$0.1–0.2, and, if C I has a like filling factor, then the C I emission is probably indeed optically thin. As the partition function of C I is well constrained, varying from its nominal value at 100 K by $\lesssim$10% for temperature uncertainties as large as a factor of 2, this yields typical beam-averaged C I column densities of about 3×10^{18} cm^{-2} through the CND, similar to extant CO column density estimates [(2–3) $\times 10^{18}$ cm^{-2}; Harris et al. 1985; Serabyn et al. 1986; Sutton et al. 1990].

However, since these CO estimates are based solely on ^{12}CO measurements, we made a check on the line opacities by measuring a few ^{13}CO 2–1 spectra toward the CND with the CSO. Comparison of these with the ^{13}CO 1–0 spectra of Zylka (1990) indicates that ^{13}CO is optically thin. A large velocity gradient (LVG) analysis of the ^{13}CO intensities, with $T_{ex} = 100$ K, a density of $\sim 10^5$ cm^{-3} in the middle to outer parts of the CND (Serabyn, Güsten, & Evans 1989), and a ^{12}CO to ^{13}CO abundance ratio of 24 (Langer & Penzias 1990) then yields a ^{12}CO column density of 4×10^{18} cm^{-2}, somewhat above the earlier estimates. Including uncertainties (temperatures 50–200 K, or densities $10^{5\pm1}$ cm^{-3}), we get a range of roughly (2–9) $\times 10^{18}$ cm^{-2}. The best estimate for the C I CO abundance ratio is then $\sim$0.8, with an error range of 0.4–1.5. This estimate can be improved when more complete isotopic CO data are available; nevertheless, the entire range is well above the typical C I/CO abundance ratio of 0.13 in molecular clouds (Keene 1990).

We now concentrate on kinematics, addressing first the $-l$ cloud. Although its nature is not clear, this cloud's location implies that "rotation curves" measured along the Galactic plane will be distorted by its presence. Indeed, low-J CO and CS lines show a roughly constant rotational velocity as a function of radius along the CND's major axis (Serabyn et al. 1986; Sutton et al. 1990), while early CO 7–6 and C II measurements seemed to imply a radial "fall-off" in velocity along the Galactic plane (Harris et al. 1985; Lugten et al. 1986). The $-l$ cloud lies in an appropriate position along the Galactic plane to account fully for this seeming discrepancy by its inclusion in the spectra (in the case of C II, the beam was large enough to be able to pick up this lower velocity emission even along the disk major axis). The $-l$ cloud is likely also responsible for the different appearances of the CND in the CO 1–0 and 3–2 lines (Serabyn et al. 1986; Sutton et al. 1990). As the CO $J = 3$–2 emission tends to be weighted more to the Galactic plane, there may well exist differences in either excitation or opacity between the CND and the $-l$ cloud.

Given its large line width, the $-l$ cloud likely also lies within the central $\sim$150 pc of our Galaxy (Güsten 1989), and it is of course entirely possible that this cloud lies as close to the center as the CND. However, since the $-l$ cloud lies at a significantly higher Galactic latitude than the CND at comparable longitudes, it would then need to lie on quite a different orbit. One possibility, which could also explain the excitation differences between this clump and the CND, is that the $-l$ cloud is a separate clump or filament which lies well above the average plane of the CND, on a highly inclined orbit, and so is more directly exposed to UV radiation from the Galactic center than the bulk of the in-plane disk. This tentative suggestion can of course only be evaluated by additional observation.

Having resolved this extraneous clump from the CND, what is left is a completely unobstructed view of the CND's southern half, allowing for a detailed examination of the gas motions out to the CND's periphery. If the motions are circular, the rotational velocity in the outer parts of the disk can then be used to constrain the central gravitational potential at these radii. To investigate the motions in the CND, we first modeled it numerically as a flat disk with six radius-independent parameters: inner and outer radii r_i and r_o, respectively, thickness t; inclination i; rotational velocity v_{rot}; and intrinsic line width f.

The best-fit model for this case of purely circular, radius-independent velocity compares very well with the observed position-velocity plot (Fig. 3). At radii $r \gtrsim 1'$, emission is seen from the tangent points, at velocities near $v_{rot} \sin i$. In this regime, the observed velocity centroids rise slightly with radius, and the observed line width decreases. Both of these effects can be attributed to decreasing kinematic smearing in our beam toward larger radii. Inside of $r \sim 1'$, the roughly constant-velocity tangent point emission fades (implying an inner radius cutoff to the disk), to be replaced by an inclined, roughly linear arm of emission which points toward the origin, and which arises from our beam subtending emission from the disk's inclined inner edge. Since this "zero-crossing branch" grows very weak toward the origin, our beam is evidently quite small in comparison with the semiminor axis of the projection onto the sky plane of the inclined disk's central cavity. These considerations lead to the following best-fit parameters: $r_i = 55''$, $r_o = 170''$, $t = 40''$, $i = 75°$, $v_{rot} = 120$ km s^{-1}, and $f = 20$ km s^{-1}. In linear units, $r_i = 2.3$ pc, $r_o = 7$ pc, and $t = 1.7$ pc. Note that r_i is substantially greater than the radius of the CND's ionized inner rim (1.4 pc; Serabyn & Lacy 1985), implying the existence of a C II zone between radii of 1.4 and 2.3 pc.

Because the overall agreement between this model and the data is quite good, there is no compelling reason to consider additional parameters describing, e.g., radial or vertical motions, or to generalize to parameters which are functions of radius, until the C I map of the CND is completed. Inclusion of a slight radial velocity component ($v_r \lesssim 15$ km s^{-1}) did seem to improve the match to the zero-crossing branch, but because clumpiness may well be distorting the otherwise smooth position-velocity diagram to a similar level, this v_r cannot be considered significant, and the limit of 15 km s^{-1} should only be considered as reflective of the level of possible divergences from the planar circular orbit case. Circular rotation of a flattened disk evidently provides a very good description of the CND kinematics. However, as evidenced by Figures 1–3, the disk is quite clumpy, and may in fact be only partially "filled."

As can be seen in Figure 4, which compares the C I rotation curve with data from other high-resolution tracers of the CND, the C I–derived rotational velocity of 120 km s^{-1} is higher than all previous estimates by about 10 km s^{-1}. Because the C I line widths are by far the narrowest in this compendium, and, furthermore, because the CO and HCN lines probably all have high opacities, the C I rotation curve is clearly the most accurate. On the other hand, allowing for beam smearing, all of the data *are* consistent with $v_{rot} = 120$ km s^{-1}, as can be seen from the plotted error bars in Figure 4. For CO and C I, which have been analyzed with models that include the effects of turbulent line broadening and beam smearing, the error bars refer to the dominant remaining source of uncertainty, the disk inclination. For the broader inner-disk lines ($\sim$50 km s^{-1} FWHM for Ne II, and 50–70 km s^{-1} for HCN), the estimated rotational velocities stem only from measurements of the line

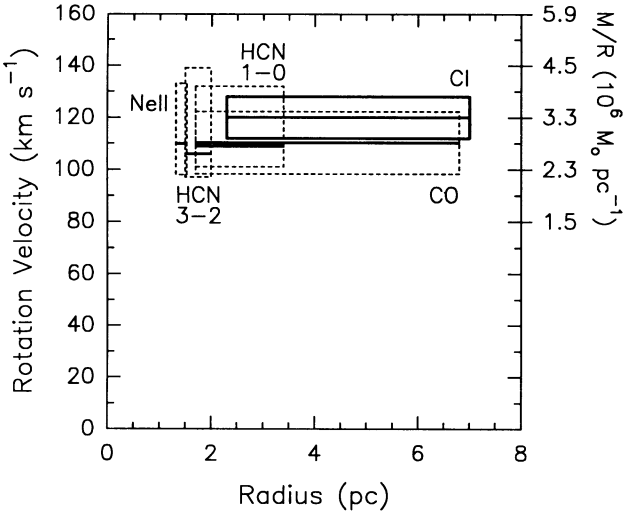

FIG. 4.—Rotational velocity vs. radius implied by extant observations of the CND kinematics. The rotational velocity is given by the solid horizontal lines, and the dotted rectangles give the error bars for each (except for C I, where the error bar box is also solid). The C I box is from this work, CO from Serabyn et al. (1986) and Sutton et al. (1990), HCN from Güsten et al. (1987) and Jackson et al. (1993), and [Ne II] from Serabyn & Lacy (1985). The right-hand scale converts the observed velocities to M/R values for the spherically symmetric case.

centroids, which of course are underestimates owing to beam smearing. As a means of showing this graphically, the upper and lower error bars for these lines are different: the lower error bar refers, as before, to the uncertainty in i, while the upper error bar is the 1 σ line width, in a Gaussian sense, of the observed line profiles. Clearly, when allowance is made for underestimation in the inner region, all of the data are consistent with the best current estimate of 120 km s^{-1}.

This C I rotation curve can be related to the central gravitational potential under various assumptions. First we consider the spherically symmetric case, which probably is an over-simplification (Becklin & Neugebauer 1968) but allows for a discussion of radial dependences. In order to keep uncertainties in the distance to the Galactic center from creeping in, the results are best presented in terms of enclosed mass divided by radius, M/R, which is simply equal to $v_{\rm rot}^2/G$ (with G the gravitational constant) in the spherical case. From the roughly radius-independent C I rotation velocity, which is consistent, within the errors, with both an isothermal stellar distribution ($M \propto R$), and the stellar cluster's IR luminosity distribution ($M \propto R^{1.2}$; Becklin & Neugebauer 1968), we get $M/R \approx (3.3 \pm 0.5) \times 10^6\ M_\odot\ {\rm pc}^{-1}$, between radii of 2.3 and 7 pc (Fig. 4). This M/R is somewhat higher than the earlier CO-based estimate at similar radii (Serabyn et al. 1986) because of the higher velocities seen in C I, and implies an enclosed mass of about $(23 \pm 5) \times 10^6$ interior to the disk's outer rim at 7 pc. If now the nonsphericity of the central stellar cluster is allowed for (Becklin & Neugebauer 1968; Sanders & Lowinger 1972), the derived M/R would have to be scaled downward by a factor approaching $\frac{1}{2}$.

Extrapolating inward, the linear mass distribution implied by the constant rotational velocity at first sight seems to leave no room for a central point mass. However, this conclusion would be incorrect, because the CND measurements at $r_{\rm pc} \geq 2.3$, cannot distinguish, in the spherically symmetric case, between different distributions at small radii (Newton 1687). Specifically, given the existence of a flattened central core in the stellar distribution (Rieke & Rieke 1988; Eckart et al. 1993), our linear mass curve cannot be extrapolated beyond the core radius. As the core appears to have a radius of $\lesssim 0.6$ pc, a central mass of up to $\sim 2 \times 10^6\ M_\odot$ would not contradict the CND kinematics. Thus, more complete measurements of the CND kinematics, together with a definitive measurement of the cluster core radius, may eventually provide a powerful technique for constraining the purported central mass.

Research at the CSO is supported by NSF grant 90-15755. We thank M. Pahre for assisting with the observations, and J. H. Lacy, A. I. Harris, and the anonymous referee for helpful comments.

REFERENCES

Becklin, E. E., & Neugebauer, G. 1968, ApJ, 151, 145
Brown, R. L., & Liszt, H. S. 1984, ARA&A, 22, 223
Eckart, A., Genzel, R., Hofmann, R., Sams, B. J., & Tacconi-Garman, L. E. 1993, ApJ, 407, L77
Gatley, I., Jones, T. J., Hyland, A. R., Wade, R., Geballe, T. R., & Krisciunas, K. 1986, MNRAS, 222, 299
Genzel, R. 1989, in IAU Symp. 136, The Center of the Galaxy, ed. M. Morris (Dordrecht: Kluwer), 383
Genzel, R., & Townes, C. H. 1987, ARA&A, 25, 377
Genzel, R., Watson, D. M., Crawford, M. K., & Townes, C. H. 1985, ApJ, 297, 766
Güsten, R. 1989, in IAU Symp. 136, The Center of the Galaxy, ed. M. Morris (Dordrecht: Kluwer), 89
Güsten, R., Genzel, R., Wright, M. C. H., Jaffe, D. T., Stutzki, J., & Harris, A. I. 1987, ApJ, 318, 124
Harris, A. I., Jaffe, D. T., Silber, M., & Genzel, R. 1985, ApJ, 294, L93
Jackson, J. M., Geis, N., Genzel, R., Harris, A. I., Madden, S., Poglitsch, A., Stacey, G. J., & Townes, C. H. 1993, ApJ, 402, 173
Keene, J. B. 1990, in Carbon in the Galaxy: Studies from Earth and Space, ed. J. C. Tartar, S. Chang, & D. J. DeFrees (NASA CP-3061), 181
Langer, W. D., & Penzias, A. A. 1990, ApJ, 357, 477
Lo, K. Y. 1989, in IAU Symp. 136, The Center of the Galaxy, ed. M. Morris (Dordrecht: Kluwer), 527
Lugten, J. B., Genzel, R., Crawford, M. K., & Townes, C. H. 1986, ApJ, 306, 691
McGinn, M. T., Sellgren, K., Becklin, E. E., & Hall, D. N. B. 1989, ApJ, 338, 824
Newton, I. 1687, Principia Mathematica
Phillips, T. G., & Huggins, P. J. 1981, ApJ, 251, 533
Rieke, G. H., & Rieke, M. J. 1988, ApJ, 330, L33
Sanders, R. H., & Lowinger, T. 1972, AJ, 77, 292
Serabyn, E., & Güsten, R. 1986, A&A, 161, 334
Serabyn, E., Güsten, R., & Evans, N. J., II, 1989, in IAU Symp. 136, the Center of the Galaxy, ed. M. Morris (Dordrecht: Kluwer), 417
Serabyn, E., Güsten, R., Walmsley, C. M., Wink, J. E., & Zylka, R. 1986, A&A, 169, 85
Serabyn, E., & Lacy, J. H. 1985, ApJ, 293, 445
Sutton, E. C., Danchi, W. C., Jaminet, P. A., & Masson, C. R. 1990, ApJ, 348, 503
Walker, C., Kooi, J. W., Chan, M., LeDuc, H. G., Schaffer, P. L., Carlstrom, J. E., & Phillips, T. G. 1992, Int. J. Infrared Millimeter Waves, 13, 785
Zylka, R. 1990, Ph.D. thesis, Univ. Bonn